

# Majorana bound states in nanowire junctions without topological superconductivity

Pablo San-Jose<sup>1</sup>, Jorge Cayao<sup>1</sup>, Elsa Prada<sup>2</sup> and Ramón Aguado<sup>1</sup>

<sup>1</sup>*Instituto de Ciencia de Materiales de Madrid (ICMM-CSIC), Cantoblanco, 28049 Madrid, Spain*

<sup>2</sup>*Universidad Autónoma de Madrid, Cantoblanco, 28049 Madrid, Spain*

(Dated: May 1, 2022)

We show that open normal-superconductor junctions in topologically trivial semiconducting wires may host fully localized Majorana bound states. The emergence of Majorana bound states in the topologically trivial regime requires a helical normal side and sufficiently transparent contact, and is a consequence of the existence of a degeneracy in the complex poles of the scattering matrix. Mathematically, this degeneracy is an exceptional point (namely a non-hermitian degeneracy that may occur in open quantum systems, at which both the eigenvalues and eigenstates coalesce). The properties of these ‘exceptional’ Majoranas are derived from those of the exceptional point. These include exact zero-energy, self-conjugation and  $4\pi$ -periodic braiding. Thus, exceptional Majoranas are the open-system counterparts of conventional Majorana bound states, and share all their peculiar properties and phenomenology, while not requiring a non-trivial bulk topology.

Since their conception in 1937<sup>1</sup>, Majorana fermions, relativistic particles that are their own antiparticles, have been the subject of intense research in the context of particle physics and cosmology<sup>2</sup>. They have long been considered as a possible description for neutrinos, and even dark matter, but a definite detection of Majorana fermions in nature has until recently eluded us. During the last few years, this state of affairs has changed, following the key observation that emergent quasiparticles in superconductors can be described as Majorana fermions<sup>3,4</sup>.

The first condensed matter proposals where this idea was put forward predicted the formation of zero energy states with Majorana character in spinless p-wave superconductors<sup>5,6</sup>. These exotic superconductors realize a topologically non-trivial electronic phase. The Majorana zero modes are expected to appear at sample boundaries in one dimension<sup>7</sup> or at vortices in two dimensions<sup>8</sup>, and are a direct consequence of this non-trivial topology. They have remarkable properties, such as non-Abelian (instead of fermionic) exchange statistics, hence the name Majorana bound states (MBSs) as opposed to Majorana fermions, and have been proposed as a basis for topologically-protected quantum computation<sup>9</sup>.

Although these p-wave superconductors are scarce in nature<sup>10</sup>, it was soon found that topological superconductors can also be engineered from the combination of various materials with conventional bulk s-wave superconductors<sup>11–14</sup>, that are themselves topologically trivial. The key was the realisation that s-wave pairing induced onto helical bands (i.e. bands in which spin polarization is correlated to momentum) behaves as effectively p-wave<sup>15</sup>. Experimental progress has been made in such implementations, particularly using semiconducting nanowires with strong spin-orbit coupling<sup>16</sup>, or the edge states of quantum spin Hall insulators<sup>17,18</sup>. Promising signatures of MBSs in the form of zero bias anomalies (ZBAs) in transport have been reported, although the measurements are still not conclusive, since ZBAs of Majorana origin can be masked or even mimicked by other physical mechanisms<sup>19–31</sup>. Less ambigu-

ous tests have been proposed in specific systems, such as non-Abelian braiding<sup>32,33</sup>, the anomalous  $4\pi$ -periodic Josephson effect<sup>7,34,35</sup>, or charge sensing<sup>36,37</sup>. All of these effects probe different aspects of MBSs, from their anyon statistics, their half-fermion character or their defining particle-hole self-conjugation. Unfortunately, conclusive experimental evidence of this stronger phenomenology is still absent.

In all of these strategies for generating MBSs, the core challenge has been to synthesise a topologically non-trivial superconductor with a well-defined gap. This is arguable the main difficulty of the original proposal<sup>13,38</sup>. In this work we propose an alternative scheme for the creation of MBSs that does not require topological superconductivity. It is based on normal-superconductor (NS) junctions fabricated in topologically *trivial* proximised semiconductor wires. Such a wire will not generate MBSs when terminated with vacuum, i.e. at a closed boundary. However, a good contact with a normal wire constitutes a different kind of *open* boundary, and may be host to zero-energy quasibound states that cannot be described using the conventional band topology language. Ultimately, these are a consequence of the existence of an exceptional point<sup>39–42</sup> in the open system, i.e. a point in which both eigenmodes and their eigenenergies in complex plane (real frequencies and decay rates) coalesce. These eigenmodes are quasi-bound, but become pinned to zero (real) energy. We identify a regime, with a helical normal side but arbitrarily far from a bulk topological transition, in which these states become genuine Majorana bound states, with all their associated phenomenology, including ZBA, fractional Josephson effect, and spatially homogeneous charge patterns. In fact, we show that these ‘exceptional’ MBSs are the open-boundary version of MBSs of topologically non-trivial wires, to which they are continuously connected. We argue that creating the conditions required for exceptional MBSs is experimentally simpler than reaching the bulk topological transition, thus providing a more flexible route towards the creation of MBSs.

**Two points of view on topology.**

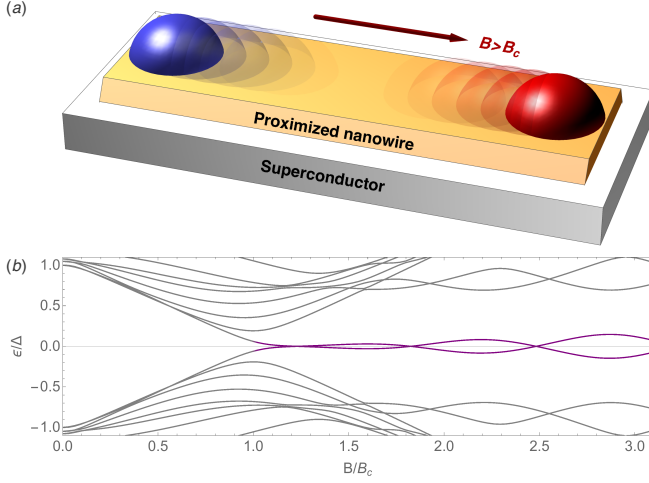


FIG. 1. (a) A finite-length semiconductor nanowire, proximized by a trivial s-wave superconductor, develops weakly overlapping Majorana bound states at its ends (blue and red) under a Zeeman field exceeding the critical  $B_c$ . (b) The spectrum of the wire in this regime has pairs of approximate zero modes, with a small splitting that oscillates with  $B$  but decreases when increasing the length of the wire (purple lines).

The concept of band topology, and transitions thereof, dates back to the 1970s<sup>43</sup>. In its simplest form it is defined in infinite periodic systems, for which sub-bands exist in a compact Brillouin zone. In a quasi-1D wire, sub-bands are a function of wavenumber  $k_x \in [-\pi/a, \pi/a]$ , where  $a$  is the wire lattice constant. A given non-degenerate subband with eigenvalues  $\epsilon(k_x)$  and eigenstates  $|\psi(k_x)\rangle$  has a topological charge (or topological invariant) given, for the so called D symmetry class in 1D,<sup>44</sup> by  $\nu = \mathcal{C} \bmod 2$ .<sup>45,46</sup> Here  $\mathcal{C}$  is the first Chern number (or normalized Zak phase<sup>47</sup>) of the subband, defined as

$$\mathcal{C} = \frac{1}{2\pi i} \int_{-\pi/a}^{\pi/a} dk_x \langle \psi(k_x) | \partial_{k_x} \psi(k_x) \rangle$$

This Chern number is a well defined integer in the absence of band crossings (*gapped* subbands). It can therefore only change value when subbands cross, or reconnect, as an external parameter is varied (band inversion).

A sketch of the nanowire proposal for topological superconductors<sup>13,38</sup> is depicted in Fig. 1. It is designed to undergo a bulk topological transition from  $\nu = 0$  to  $\nu = 1$  when the Zeeman splitting  $B = \frac{1}{2}g\mu_B|\vec{B}|$  (with a magnetic field  $\vec{B}$  aligned along the wire) exceeds a critical value  $B_c = \sqrt{\mu_S^2 + \Delta^2}$  ( $\mu_S$  and  $\Delta$  are the wire's Fermi energy and induced gap respectively). An interface between a  $B > B_c$  semi-infinite wire (with  $\nu = 1$ ) and vacuum ( $\nu = 0$ ) binds a single subgap state (for D-class in 1D)<sup>45,46</sup>. The state is pinned to zero energy by the particle-hole symmetry of the Bogoliubov-de Gennes description, locked strictly midway between electrons and holes; it satisfies the Majorana condition  $\gamma = \gamma^\dagger$ , and is

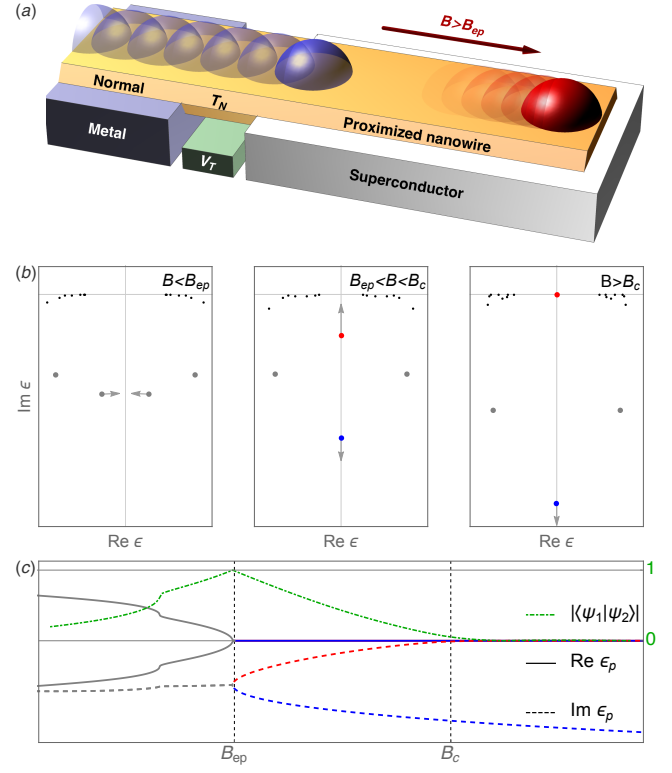


FIG. 2. (a) A proximized nanowire such as in Fig. 1, contacted to a normal reservoir through a junction of tunable transparency. Such open system develops two zero energy quasibound states after crossing an exceptional point ( $B > B_{ep}$ ), one of which evolves into an approximate Majorana bound state (red) for  $B > B_c$ . This pole transition and topological crossover may be visualised in the poles of the junction's scattering matrix (b), which exhibit a bifurcation and burying into the origin at  $B_{ep}$  and  $B_c$  respectively, panel (c). The dashed-dotted green line denotes the overlap of the coalescing eigenmodes, that reaches one at  $B_{ep}$ .

hence known as a MBS. This robust pinning is broken when two MBSs are brought within a finite distance of each other, i.e. in a topological nanowire of finite length  $L_S$ , see Fig. 1. Both MBSs then hybridize into a single conventional fermion of finite energy, or Andreev bound state. The energy splitting can be small for long enough wires (see purple lines in Fig. 1b), though strictly speaking it is non-zero for any length<sup>28,48–50</sup>. The MBSs become merely quasi-stationary states, with their energy splitting representing a Rabi frequency at which one oscillates into the other. The analysis of MBSs formation in terms of band topology breaks down, as it cannot incorporate a finite system size, and a different point of view on system topology becomes necessary.

One such alternative was developed by Pikulin and Nazarov,<sup>51,52</sup> who studied the topological properties of the scattering matrix (S-matrix) for interfaces between a normal reservoir and a superconductor, see Fig. 2a, as opposed to band topology of infinite gapped systems. This approach is arguably the most general formulation

one can devise to characterize the topological properties of finite size nanostructures. In this language, all information about the system is encoded into the poles  $\epsilon_p$  of the S-matrix  $S(\epsilon)$ , which lie in the lower complex energy plane. Such complex poles have a well defined physical interpretation that generalises the eigenstates of closed wires. They define quasi-bound states in the superconducting junction, with their real part  $\text{Re } \epsilon_p$  representing finite energy away from zero while their imaginary part  $\text{Im } \epsilon_p$  representing their inverse lifetimes, caused by escape into the reservoirs. Particle-hole symmetry of the superconducting system dictates that, for each pole at  $\epsilon_p$ , there must exist another at  $-\epsilon_p^*$ , located symmetrically at the opposite side of the imaginary axis (i.e. with identical imaginary part). In general this symmetry groups poles in pairs, *unless* they lie exactly along the imaginary axis, in which case they can be unpaired but are then locked to have  $\text{Re } \epsilon_p = 0$ .

Pikulin and Nazarov showed that topology classes for the S-matrix can be defined in terms of the number  $N_Y$  of such poles, i.e. with zero real part but finite imaginary part. S-matrices with even  $N_Y$  (trivial) and odd  $N_Y$  (non-trivial) were shown to be topologically inequivalent, and to correspond to the cases  $\nu = 0$  and  $\nu = 1$  of semi-infinite systems in the tunneling junction limit. Due to the particle-hole symmetry of its poles, however, the  $N_Y$  of physical finite length systems can only change with external parameters by  $\pm 2$  (no change in the parity of  $N_Y$ ), when a pair  $\epsilon_p$  and  $-\epsilon_p^*$  meets at the imaginary axis. The fusion of the two poles is known as a “pole” transition.

A pole transition is a particular instance of a more general phenomenon, known in the field of open quantum systems as an exceptional point. It is a point in parameter space in which an open system, described by a non-Hermitian operator, has two (or more) degenerate eigenvalues in the complex plane. A simple example is the transition of an oscillator from underdamped to overdamped. The consequences of the existence of an exceptional point are far-reaching, and imply e.g. a non-trivial geometrical phase of the corresponding eigenmodes, similar to the Berry phase of Hermitian systems<sup>42,53</sup>. As opposed to closed systems described by hermitian Hamiltonians, the degenerate eigenstates at an exceptional point are not orthogonal, but coalesce as the eigenenergies themselves. In our particular system, the exceptional point occurs at a certain  $B = B_{ep}$ , as shown in Fig. 2(b,c), above which the imaginary part of the two fusing poles bifurcate (one increases while the other decreases). The coalescence of the two eigenstates corresponding to the poles is demonstrated through their overlap, which reaches one at the exceptional point, see dashed-dotted line in Fig. 2c.

The imaginary part of one of the  $N_Y$  poles may become very small after the bifurcation. An instance of this process was discussed in Ref. 51 and 52, and was termed “pole burying”. This process was shown to take place around  $B \approx B_c$  in finite-length wires, and replaces

the topological transition of semi-infinite wires, which becomes a “topological crossover” instead. In this context, the buried pole corresponds to a state spatially well localised at the end of the wire away from the contact (red sphere in panel a, and right panel in Fig. 2b). The pole asymptotically approaches the origin but never truly reaches it, which marks the difference between a proper topological transition and a crossover. Hence  $N_Y$  does not change in the crossover, and the S-matrix remains trivial, rigorously speaking. A trivial S-matrix with an odd number of buried poles will, however, exhibit effectively non-trivial phenomenology, and the states associated to said poles will behave as true MBSs, provided their lifetimes are longer than any other timescale in the problem. This is analogous to the case of a finite- $L_S$  isolated nanowire at  $B > B_c$ , with a small enough splitting of the two MBSs, except that the residual energy is then a real frequency instead of a decay rate.

In the following we show that by tuning the properties of the contact and the carrier concentrations, one may control the occurrence of the exceptional point, the S-matrix topological crossover and the lifetime of the buried poles. Our main result is that an effectively non-trivial S-matrix can be realised much before the bulk topological transition ( $B_{ep} < B \ll B_c$ ), after crossing the exceptional point. This lead to the emergence of an exceptional MBS deep in the trivial regime ( $B \ll B_c$ ). Unlike its  $B > B_c$  counterpart, the exceptional MBS is located at the open NS junction, but has also a vanishing decay rate, i.e. it is a junction ‘dark’ state. The basic conditions that must be fulfilled are (i) a sufficiently transparent contact, (ii) a normal side in the helical regime (low electron density), and (iii) a superconducting side in the Andreev limit (high electron density).

## Results

### Exceptional points and Majorana resonances.

We now illustrate the concept of an exceptional point and the generation of Majorana resonances in a nanowire NS junction. Majorana resonances are the finite-lifetime zero-energy states (lying on the imaginary axis) that emerge from the bifurcation at an exceptional point, and will be shown to be precursors of exceptional MBSs. We consider the ideal case, depicted in Fig. 2a, of a single channel InSb nanowire close to depletion, with its right side, of length  $L_S$ , proximized with a pairing  $\Delta$ . The left side is open to a reservoir, while the wire is closed on the right. The Fermi energy is small and uniform  $\mu_N = \mu_S \lesssim \Delta$ , and the NS contact has a normal  $B = 0$  transparency per channel  $T_N$  that may be externally tuned (e.g. through a pinch-off barrier). This setup allows us to explore the evolution between an isolated finite-length superconducting nanowire for  $T_N \rightarrow 0$  to a perfectly open nanowire for  $T_N = 1$ . By computing the poles of the scattering matrix and the local density of states (LDOS) at the NS interface, we may correlate the appearance of a Majorana zero-energy resonance at the contact to the exceptional point as  $T_N$  is increased.

The results are shown in Fig. 3 (see parameter val-

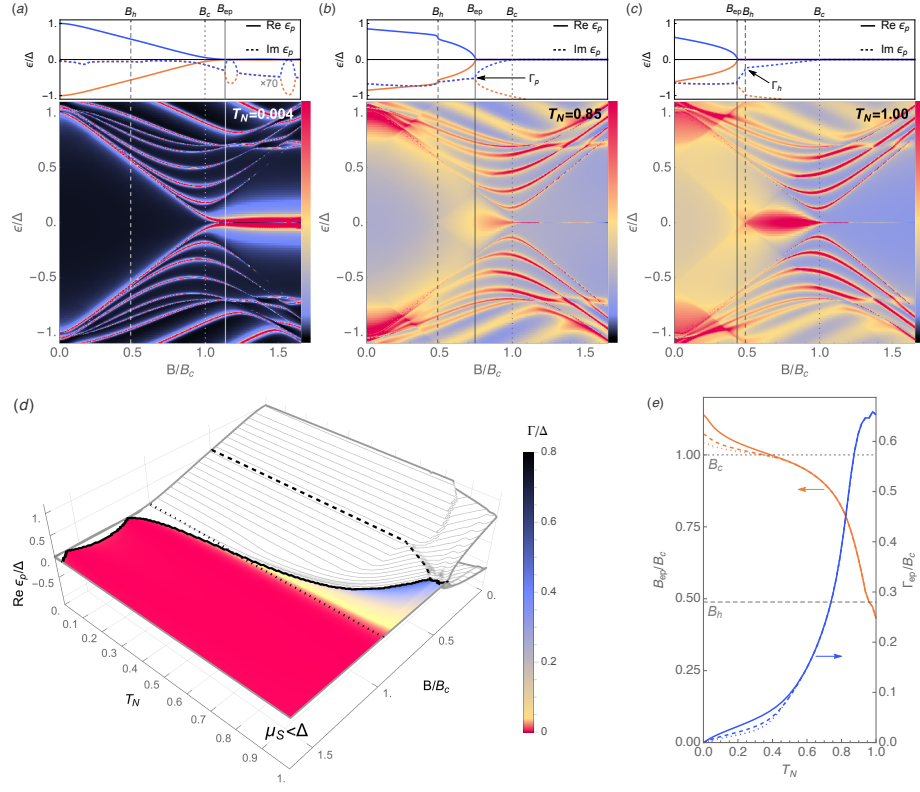


FIG. 3. (a-c) Local density of states at the NS contact in a InSb nanowire with spin-orbit coupling  $\alpha = 20$  meV nm, g-factor  $g = 40$ , a uniform Fermi energy  $\mu_N = \mu_S = 0.14$  meV, and an induced pairing  $\Delta = 0.25$  meV on its right portion, of length  $L_S = 1.5\mu\text{m}$ . The three panels correspond to increasing contact transmission per channel,  $T_N = 0.02, 0.85$  and  $1.0$ . Thin guidelines correspond to the pole transition field  $B_{ep}$  (solid), helical  $B_h = \mu_N = 0.12$  T (dashed) and critical  $B_c = \sqrt{\mu_S^2 + \Delta^2} = 0.25$  T (dotted). Top plots show the evolution of the real and imaginary part of the two lowest poles of the scattering matrix, which exhibit a pole transition at  $B_{ep}$  defined by  $\text{Re } \epsilon_p = 0$ , and a bifurcating inverse lifetime  $\Gamma = \text{Im } \epsilon_p$ . This bifurcation is shown in the full  $T_N$ - $B$  plane in (d). Red regions host MBSs, while yellow regions contain Majorana resonances. Panel (e) shows the pole transition field  $B_{ep}$  for increasing contact transmission, and the corresponding bifurcation  $\Gamma_{ep}$  at  $B = B_{ep}$ . Solid, dashed and dotted curves correspond to increasing lengths of the proximised nanowire section  $L_S = 1.5\mu\text{m}$ ,  $3.0\mu\text{m}$  and  $4.5\mu\text{m}$ .

ues in caption). Panels (a-c) show the LDOS (bottom plots) and the evolution of the lowest poles of the S-matrix (top plots) for different transparencies  $T_N$ , while panel (d) shows the bifurcation of these poles in the full  $T_N$ - $B$  plane. Panel (a) corresponds to the tunnelling limit  $T_N \ll 1$ , which exhibits a sharp peak at zero-energy due to conventional MBSs for  $B \gtrsim B_c$ , slightly split in two due to their hybridization across  $L_S$ . As  $T_N$  is increased (Figs. 3[b,c]), the  $B \gtrsim B_c$  zero-energy peak in the LDOS is washed away, since the Majorana at the contact becomes a finite-lifetime Majorana resonance, increasingly delocalized into the reservoir.

Interestingly, however, the onset of the Majorana resonance is shifted to fields  $B < B_c$ , for which the band topology of the superconducting nanowire is trivial. The Majorana resonance emerges upon crossing an exceptional point at a certain  $B_{ep}$  (see bifurcation of the two lowest scattering matrix poles in the top plots in Fig. 3[a-c], and in Fig. 3d). Fig. 3e shows the evolution of  $B_{ep}$  for different wire lengths, together with the resonance width

$\Gamma_{ep} = -\text{Im } \epsilon_p$  taken at the exceptional point (see arrow in panel [b], thick line in panel [d]). As  $T_N$  is increased from 0 to 1,  $B_{ep}$  decreases from  $B_{ep} \approx B_c$  (solid guidelines) to  $B \approx B_h$  (dashed), where  $B_h \equiv \mu_N$  is the field for which the N side of the junction becomes helical, and loses one propagating channel.

Two important conclusions can be drawn from these results. On the one hand, we see that the topological transition and the exceptional point coincide,  $B_{ep} = B_c$ , in the particular  $T_N \rightarrow 0, L_S \rightarrow \infty$  limit.<sup>52</sup> For wires sufficiently open to reservoirs, however, the exceptional point and its associated Majorana resonance will occur at lower fields (around  $B_h$ ) than the topological crossover, or pole burying (at  $B_c$ ), and might therefore be easier to reach experimentally. Secondly, the difference between a Majorana resonance at  $B < B_c$  and a conventional  $B > B_c$  MBSs in *finite* wires seems to be merely qualitative, i.e. differing simply in their lifetime, since both correspond to the same pole of the scattering matrix at different positions in the complex plane. Conventional

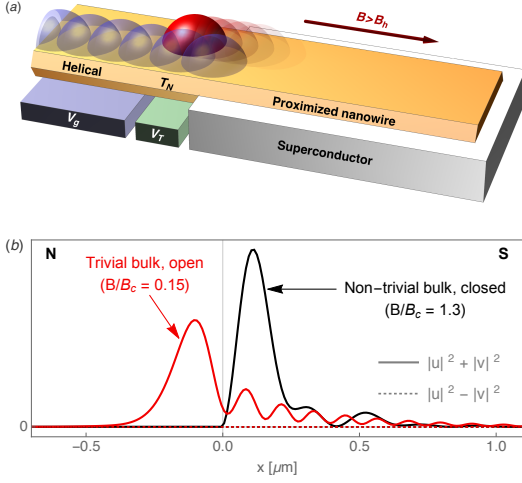


FIG. 4. (a) Sketch of a transparent  $T_N \approx 1$  NS junction hosting a MBS (red) for  $B_h < B < B_c$ , for which the normal side has an odd number of propagating modes. (b) Spatial quasiparticle density  $|u|^2 + |v|^2$  for Majorana bound states in a transparent NS junction at  $x = 0$  between trivial bulks for  $B_h < B < B_c$  (solid red [light] curve, corresponding to white arrow in Fig. 5c), and in a tunnel junction to a  $B > B_c$  finite length nanowire (solid black [dark],  $\mu_S < \Delta$  like in Fig. 3a). Dotted lines are the corresponding charge densities  $|u|^2 - |v|^2$ , zero everywhere, revealing the Majorana character of the states.

MBSs above  $B_c$  have a finite (real) energy splitting due to the finite length, while Majorana resonances below  $B_c$  have a finite width  $\Gamma$ . However, while the former can be decreased by increasing the length of the proximized wire (making the MBSs effectively eigenstates), the inverse lifetime  $\Gamma$  of Majorana resonances is always sizeable in the present regime ( $\mu_S \lesssim \Delta$ ); it decreases with Zeeman field, and exhibits a kink for high  $T_N$  at the helical transition  $B = B_h$  of the normal side (arrow in panel [c]), but it remains relatively large all the way till  $B_c$ . In the next section, we will show that in the experimentally relevant regime  $\mu_S \gg \Delta$  this is no longer the case. The kink at  $B_h$  evolves, at high  $T_N$ , into an S-matrix topological crossover far below  $B_c$ , which gives rise to the formation of a new type of exceptional MBSs at the junction, with  $\Gamma \rightarrow 0$ .

**Majorana bound states without topological superconductivity.** We have shown that Majorana resonances for  $B > B_{ep}$  evolve continuously into conventional MBSs as  $B$  crosses  $B_c$ . A natural question arises as to why a zero-energy Majorana resonance may appear in a topologically trivial wire in the first place. This may be intuitively understood by considering that a topologically trivial  $B < B_c$  isolated nanowire actually hosts a pair of MBSs pairs at each end (one for each of two opposite p-wave sectors in the trivial wire<sup>54</sup>), that are strongly hybridized away from zero energy to an energy close to  $\Delta$ , due to their large overlap. However, when one end is fully opened into a helical wire with a single propagating mode ( $B > B_h > B_{ep}$ ), one (and only one) of the

two MBSs escapes into the reservoir, and decouples from the other MBS, which remains well localized at the contact and returns to zero energy. This mechanism does not apply for  $B < B_h$  since in this case both MBSs may immediately escape into the reservoir.

This physical picture, illustrated in Fig. 4a, allows us to understand the origin of the finite lifetime of a Majorana resonance, Fig. 3e. It is connected to the probability for one of the two hybridized Majoranas to completely escape into the helical wire and out into the reservoir. The higher this probability, the longer-lived the remaining Majorana will be, since its overlap with its delocalised sibling will be suppressed. For perfect escape probability, the Majorana becomes a zero-energy, non-decaying dark state at the junction. One might guess that this escape probability should be  $T_N$  itself, but we showed in Fig. 3 that a  $T_N = 1$  contact with  $\mu_S \lesssim \Delta$  has a Majorana resonance of finite lifetime. The reason is that a perfect normal transparency  $T_N = 1$  only implies escape probability one across the NS junction in the limit in which the induced pairing  $\Delta$  is a small perturbation respect to the normal phase, i.e. in the Andreev limit  $\mu_S \gg \Delta$ . This is, incidentally, the realistic regime of experimental samples, since electrostatically depleting a proximized wire to have  $\mu_S \lesssim \Delta$  is much more difficult than depleting an exposed section, whose  $\mu_N$  can typically be tuned all the way to zero by a gate.

To demonstrate this scenario, we show in Fig. 5 the LDOS and pole evolution of the NS junction in the Andreev limit. We have taken all parameters as in the simulation of Fig. 3, except for a  $\mu_S = 10\Delta$ . This moves the topological crossover  $B_c$  to higher fields ( $B_c = 2.2$  T, up from 0.25 T), while the helical field  $B_h = \mu_N$  (dashed guideline) remains the same. The range of physical  $B$  fields is the same as in Fig. 3, but now  $B_c$  falls outside of this range.

As  $T_N$  is increased (by making the spatial transition between  $\mu_N$  and  $\mu_S$  at the contact smooth<sup>55</sup>), the width of the Majorana resonance becomes greatly reduced, i.e. the resonance becomes gradually decoupled from the reservoir. Note the similarity between the sharp zero energy peak in the LDOS emerging in Fig. 5c at  $B_h$  and the one in Fig. 3a for  $B > B_c$ . The width of the latter, a conventional MBSs associated to a topologically non-trivial superconducting bulk, vanishes as  $T_N \rightarrow 0$ . The width of the former, in contrast, decreases towards  $\Gamma = 0$  as  $T_N \rightarrow 1$  and  $\mu_S/\Delta$  is increased. This is demonstrated in Fig. 5c, which shows  $\Gamma_h = -\text{Im} \epsilon_p$  at the helical transition  $B_h$  for  $T_N \approx 1$  as a function of  $\mu_S/\Delta$ . We see that  $\Gamma_h$  is quickly suppressed as soon as we approach the Andreev limit  $\mu_S > \Delta$ , and becomes arbitrarily small as  $\mu_S$  grows. This supports the intuitive picture of the preceding paragraphs.

Finite-length proximized wires acquire effectively non-trivial topology at  $B_c$  through a pole burying of the S-matrix (top plots in Fig. 3). Exactly the same pattern is replicated here in the Andreev limit for an open NS junctions at  $B_h$  (black arrow in Fig. 5c). By the S-matrix def-



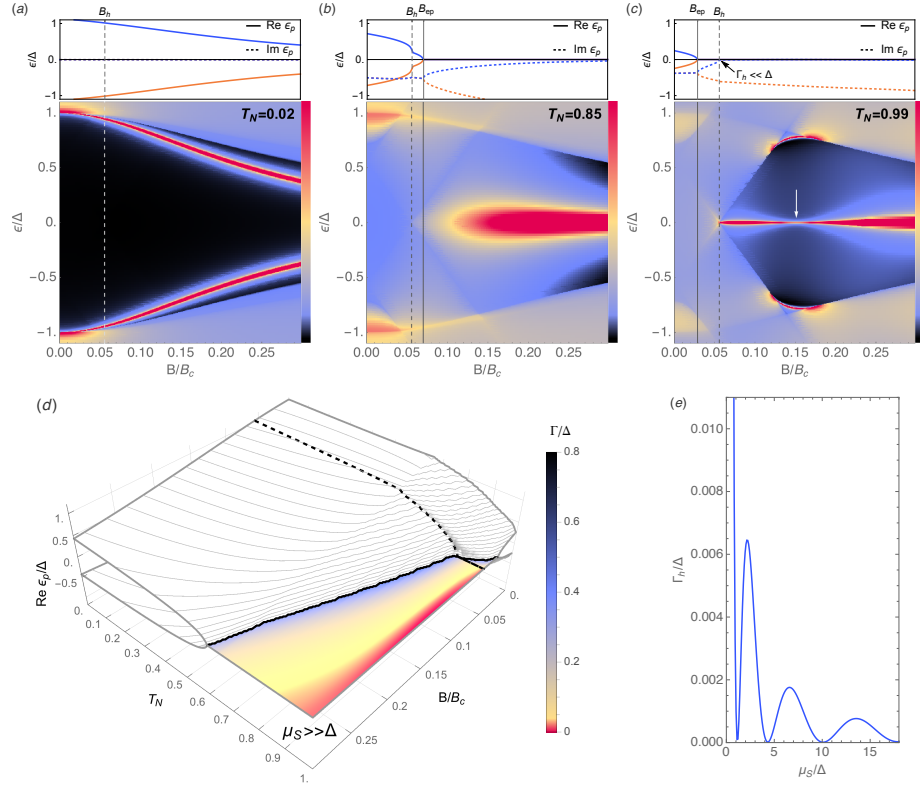


FIG. 5. (a-c) Local density of states in NS junctions in the Andreev limit  $\mu_S \gg \Delta$ . All parameters and plot ranges are like in Fig. 3, except for  $\mu_S = 2.5\text{meV} = 10\Delta$ , so that now  $B_c = 2.1$  T (outside of plotted range). The pole bifurcation diagram (d) shows exceptional MBSs (red) at high transparencies for  $B_c > B > B_h$ . (e) Majorana resonance inverse lifetime  $\Gamma_h$  evaluated at  $B = B_h$  for  $T_N \approx 1$  (see also black arrow in [c], top), versus the ratio  $\mu_S/\Delta$ .  $\Gamma_h$  rapidly falls to zero as the Andreev limit is reached.

initiation, the junction becomes effectively non-trivial topologically for  $B > B_h$ , while by the band topology definition, both normal and superconducting bulks remain trivial ( $B \ll B_c$ ). In spite of the system being arbitrarily far from a band topological transition, the more general S-matrix point of view shows that the zero energy state associated to the buried pole is a genuine Majorana bound state. In contrast to a  $B > B_c$  MBS, the exceptional MBS is located *at* the junction (red sphere in Fig. 4a), and its residual energy scale can be tuned all the way to zero by increasing  $T_N$  instead of  $L_S$ . In the following we will demonstrate its Majorana character, and analyse its associated phenomenology.

**Majorana phenomenology of exceptional Majorana bound states.** In this section we will further substantiate our claim that  $B < B_c$  MBSs in open junctions are indeed Majoranas, by showing that they share the physical properties expected of conventional  $B > B_c$  MBSs. In particular we demonstrate wavefunction locality, particle-hole conjugation, differential conductance in NS geometries, uniform charge oscillations and the  $4\pi$  fractional Josephson effect in SNS geometries.

The spatial locality and Majorana self-conjugation  $\gamma = \gamma^\dagger$  are assessed first, by analysing the eigenstate of the buried pole. Figure 4b shows, in red (light), the quasipar-

ticle density  $|\psi(x)|^2 = |u|^2 + |v|^2$  (solid lines) and charge density  $|\rho(x)|^2 = |u|^2 - |v|^2$  (dashed lines) of the exceptional MBS marked by the white arrow in Fig 5c ( $u$  and  $v$  are particle and hole components of its wavefunction, respectively). As discussed above, the buried pole represents a long lived state at zero energy. The figure shows that it is furthermore well localised at the junction, decaying exponentially to either side. For comparison we also show in black the spatial probability  $|\psi(x)|^2$  of a conventional  $B > B_c$  MBSs for a topological bulk at tunnel transparency. For both states, the charge density  $\rho(x)$  is zero, as implied by the Majorana relation  $\gamma = \gamma^\dagger$ .

The presence of zero-energy MBSs in a junction leads in general to zero bias anomalies in transport. In the tunneling limit, the differential conductance  $dI/dV$  as a function of bias  $V$  gives a measure of the local density of states at the contact, and is hence peaked at zero when a MBSs appears at  $B > B_c$ . This gives rise to generic Y-shaped features in the  $V$ - $B$  plane<sup>56</sup>, see Fig. 6a, with a residual splitting for  $B > B_c$  due to the finite  $L_S$ <sup>52,57</sup>. The analogous ZBA for a  $B_h < B < B_c$  MBS in the transparent limit is an inverted version of the tunneling case. Instead of a peak, the  $dI/dV$  for  $B > B_h$  exhibits a narrow dip of width  $\Gamma$  on a  $2e^2/h$  background. For  $B < B_h$ , the  $dI/dV$  is a superposition of two Zeeman-

split  $2e^2/h$  plateaux, corresponding to perfect Andreev reflection of each of the two spin sectors at the junction. The evolution from a split  $4e^2/h$  plateau to a MBS dip yields a different characteristic Y-shape feature in  $dI/dV$  that should be experimentally recognisable, see Fig. 6b.<sup>58</sup>

The next test, related to the non-Abelian braiding properties of exceptional MBSs, is to check that the pole fusion at  $B_{ep}$  is indeed an exceptional point. This is confirmed by wavefunction overlap of the two degenerate eigenstates, which in all cases reaches one at  $B_{ep}$ , similarly to Fig. 2c, dot-dashed line. Such eigenstate coalescence has been shown to give rise to Majorana-like braiding properties in the neighbourhood of the exceptional point<sup>59</sup>. These braiding processes are in general formulated as a mathematical property of exceptional points, in terms of Berry phases<sup>42</sup>. Physically, one can perform the equivalent to such a braiding process in a SQUID geometry, by checking whether the spectrum is  $4\pi$ -periodic in the phase difference across the junction. Based on parity-conservation arguments, it has been shown that the resulting  $4\pi$  Josephson effect is a strong proof of non-trivial superconductor topology.<sup>35</sup> These arguments, however, do not directly apply to open systems such as ours, where parity is not conserved. The question then arises as to whether the exceptional Majoranas could carry a  $4\pi$ -periodic Josephson current even though the host superconductor is topologically trivial. The answer is affirmative, which reinforces the interpretation that exceptional MBSs, although not-topologically protected, are indistinguishable from conventional MBSs.

The fractional Josephson test is performed in an open SQUID geometry, see inset of Fig. 7, threaded by a magnetic flux that results in a phase difference  $\phi$  across the Josephson junction. The junction is also coupled to normal reservoirs by two NS contacts that are kept open ( $T_N \approx 1$ ), each of which should therefore host an exceptional MBS for  $B > B_h$ . An additional coupling between the ends of the normal leads, of transmission  $T_J$ , is introduced, so that a persistent supercurrent (dashed line) can flow around the loop. The main contribution of this supercurrent is carried by the  $\phi$ -dependent hybridization of the two exceptional MBSs. As long as  $T_J$  is small enough, the lifetime of the exceptional MBSs should remain large, since its sibling Majorana is still strongly delocalised into the reservoir. As  $T_J$  is increased, however, the exceptional MBS should become a finite-life resonance, as in the case of  $T_N < 1$ .

Figure 7 shows the contribution to the total density of states (DOS) of the buried pole in the open SQUID (gray contours). Its derivative respect to  $\phi$  for negative energies yields the supercurrent they carry<sup>60</sup>. In panel (a)  $T_J$  is small, so that the decay rate of the MBSs remains very small, and the DOS is strongly peaked at  $\pm E\epsilon_p$  of the two hybridized exceptional MBSs (red lines). The splitting goes as  $\cos(\phi/2)$ , while the width  $\Gamma$ , thinner than the red line in the plot, is not visible. Note that there is no splitting at  $\phi = \pi$ , however small. The Josephson current

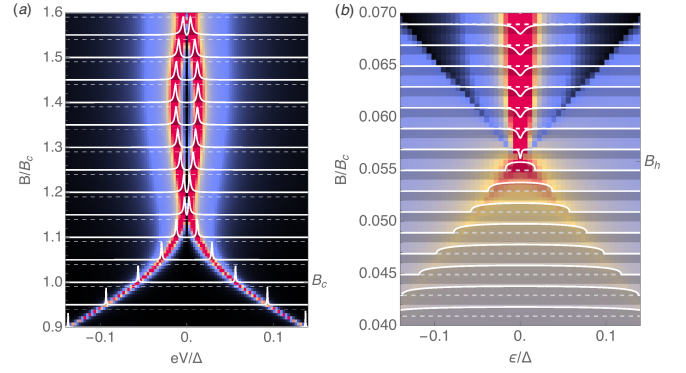


FIG. 6. Y-shaped feature in differential conductance  $dI/dV$  of an NS contact (white curves) in the tunneling limit (a) and the transparent limit (b), corresponding to portions of Figs. 3a and 5c, respectively. Dashed guidelines correspond to  $dI/dV = 2e^2/h$ . The density plot in the background corresponds to the LDOS at the contact.

is therefore  $4\pi$ -periodic. In this case, the Josephson effect is indistinguishable from that of conventional MBSs in topological Josephson junctions, and is a direct demonstration of non-trivial braiding of exceptional MBSs. We have also checked that the critical current (supercurrent at  $\phi = \pi$ ) scales as  $\sqrt{T_J}$  for small  $T_J$ , which is also a characteristic Majorana feature. The case of larger  $T_J$ , panel b, deviates from this general picture. While the splitting is still zero at  $\phi = \pi$ , it is also zero within a window around this value. The same happens if  $T_N < 1$ . The phase difference  $\phi$ , in this case, produces a double pole transition around  $\pi$ . The increased  $T_J$ , however, also reduces the lifetime of the exceptional MBSs (see finite width of gray contours), which implies that a  $4\pi$ -periodicity should only manifest in fast transients in this case<sup>61</sup>, much like in finite-length topological nanowires.

To finish our analysis of Majorana phenomenology, we examine the charge density patterns that arise from the weak overlap of two exceptional MBSs. It was shown<sup>37</sup> that the charge density  $\rho(x) = |u|^2 - |v|^2$ , which is zero everywhere for an isolated MBS (see Fig. 4b), develops a spatial oscillatory pattern that is uniform throughout space when two MBSs approach each other in a 1D superconductor, irrespective of their particular positions. This is a very specific and non-trivial signature of MBSs that probes the state wavefunction itself, and was proposed as a way to detect MBSs through charge sensing. A transparent NSN junction (with N portions coupled to reservoirs) provides a convenient geometry to study this effect. Two localized exceptional MBSs appear for  $B > B_h$  at the two ends of the S section. They weakly overlap, and should thus be expected to exhibit uniform spatial charge oscillation throughout the superconductor in analogy to conventional MBSs. Fig. 8 compares the charge density  $\rho(x)$  for  $B > B_c$  MBSs in the tunneling limit and  $B_h < B < B_c$  in the transparent limit. Once more, we see the strong similarity between the two cases, due to the essential equivalence between the two types of

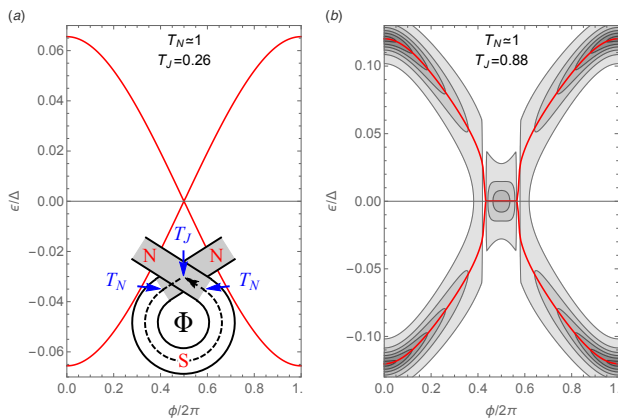


FIG. 7.  $4\pi$  Josephson effect with exceptional MBSs. The red curves are the splitting of exceptional MBSs (buried poles) across a Josephson junction between trivial superconductors (at  $B = B_h < B_c$ ), as a function of superconducting phase difference  $\phi$ . The junction is also open to helical normal leads at NS junctions of normal transparency  $T_N \approx 1$ , see inset (parameters as in Fig. 5c). Panel (a) and (b) correspond to small and large Josephson junction transmission  $T_J$ , respectively. The width (inverse lifetime) of the hybridized MBSs remains small if  $T_J$  is small (thinner than red line in panel a). Note the perfect crossing at  $\phi = \pi$  and the resulting  $4\pi$ -Josephson effect, despite the trivial topology.

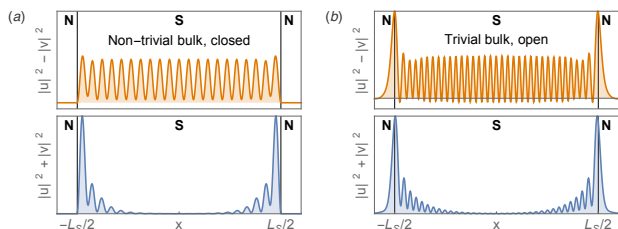


FIG. 8. Charge density  $|u|^2 - |v|^2$  and quasiparticle density  $|u|^2 + |v|^2$  at  $B = 2\Delta = 0.43$  T in an NSN wire hosting one Majorana at each junction. Panel (a) corresponds to conventional  $B > B_c$  MBSs in the tunnel limit  $T_N \approx 0$  (see Fig. 3a), while panel (b) corresponds to  $B < B_c$  in the transparent limit  $T_N \approx 1$  (see Fig. 5c). Both exhibit uniform spatial charge density oscillations.

states.

## Conclusions

We have demonstrated the possibility to engineer MBSs in an open junction between a ballistic normal and a proximised semiconducting wire, without inducing a bulk topological transition in the superconducting side. Our proposal requires creating the conditions (high contact transparency) for the emergence of an exceptional point in the system at a field  $B_{ep}$  below the helical transition  $B_h$  of the normal wire (odd number of propagating channels). The superconducting side need not be depleted as in previous nanowire proposals, and should remain in its natural Andreev limit of high densities. At large enough normal junction transparency  $T_N$ , a lone Majorana bound state then emerges at the contact for  $B > B_h$  that, although not topologically protected, has an arbitrarily long lifetime, controlled by  $T_N$ . These conditions are expected to be more accessible experimentally than the bulk topological superconducting transition required in conventional proposals for MBSs. We have furthermore showed that the properties of the resulting exceptional MBSs, derived from those of the exceptional point, are indistinguishable from those of conventional Majoranas. They share all the relevant transport and spectral phenomenology expected of conventional MBSs in one-dimensional wires, save for the associated zero bias transport anomaly, which becomes characteristically inverted.

The general connection demonstrated here between Majorana states and zero energy poles emerging from exceptional points, offers a new perspective on the mechanisms that may give rise to Majorana states in condensed matter, by extending previous approaches to open systems. Rather counter-intuitively, we have shown that opening a quantum system to its environment may prove to be the best strategy towards generating and detecting the elusive Majorana states in the lab.

## ACKNOWLEDGMENTS

We are grateful to C. W. J. Beenakker, D. Pikulin, J. Sau and A. Soluyanov for illuminating discussions. We acknowledge the support of the European Research Council and the Spanish Ministry of Economy and Innovation through the JAE-Predoc Program (J. C.), Grants No. FIS2011-23713 (P.S.-J), FIS2012-33521 (R.A.) and the Ramón y Cajal Program (E. P.).

<sup>1</sup> E. Majorana, Nuovo Cimento , 171 (1937).

<sup>2</sup> F. T. Avignone, S. R. Elliott, and J. Engel, Rev. Mod. Phys. **80**, 481 (2008).

<sup>3</sup> F. Wilczek, Nat Phys **5**, 614618 (2009).

<sup>4</sup> S. R. Elliot and M. Franz, arXiv:1403.4976 (2014).

<sup>5</sup> N. Read and D. Green, Phys. Rev. B **61**, 10267 (2000).

<sup>6</sup> G. E. Volovik and G. Volovik, *The universe in a helium droplet*, Vol. 117 (Oxford University Press New York, 2009).

<sup>7</sup> A. Y. Kitaev, Phys. Usp. **44**, 131 (2001).

<sup>8</sup> G. E. Volovik, JETP Lett. **70**, 609 (1999).

<sup>9</sup> C. Nayak, S. Simon, A. Stern, M. Freedman, and S. Das Sarma, Rev. Mod. Phys. **80**, 1083 (2008).

<sup>10</sup> K. D. Nelson, Z. Q. Mao, Y. Maeno, and Y. Liu, Science **306**, 1151 (2004), <http://www.sciencemag.org/content/306/5699/1151.full.pdf>.

<sup>11</sup> L. Fu and C. L. Kane, Phys. Rev. Lett. **100**, 096407 (2008).



- <sup>12</sup> J. D. Sau, R. M. Lutchyn, S. Tewari, and S. Das Sarma, Phys. Rev. Lett. **104**, 040502 (2010).
- <sup>13</sup> R. M. Lutchyn, J. D. Sau, and S. Das Sarma, Phys. Rev. Lett. **105**, 077001 (2010).
- <sup>14</sup> J. Alicea, Phys. Rev. B **81**, 125318 (2010).
- <sup>15</sup> For reviews, see J. Alicea, Rep. Prog. Phys. **75**, 076501, (2012); C. Beenakker, Annu. Rev. Cond. Mat. Phys. **4**, 113, (2013); T. Stanescu and S. Tewari, J. Phys. Condens. Matter **25**, 233201, (2013).
- <sup>16</sup> V. Mourik, K. Zuo, S. Frolov, S. Plissard, E. Bakkers, and L. Kouwenhoven, Science **336(6084)**, 1003 (2012).
- <sup>17</sup> S. Hart, H. Ren, T. Wagner, P. Leubner, M. Mühlbauer, C. Brüne, H. Buhmann, L. W. Molenkamp, and A. Yacoby, Nat. Phys. **10** (2014).
- <sup>18</sup> V. S. Pribiag, A. J. A. Beukman, F. Qu, M. C. Cassidy, C. Charpentier, W. Wegscheider, and L. P. Kouwenhoven, arXiv:1408.1701 (2014).
- <sup>19</sup> F. Pientka, G. Kells, A. Romito, P. W. Brouwer, and F. von Oppen, Phys. Rev. Lett. **109**, 227006 (2012).
- <sup>20</sup> D. Bagrets and A. Altland, Phys. Rev. Lett. **109**, 227005 (2012).
- <sup>21</sup> J. Liu, A. C. Potter, K. T. Law, and P. A. Lee, Phys. Rev. Lett. **109**, 267002 (2012).
- <sup>22</sup> J. D. Sau and S. Das Sarma, Phys. Rev. B **88**, 064506 (2013).
- <sup>23</sup> E. J. H. Lee, X. Jiang, M. Houzet, R. Aguado, C. M. Lieber, and S. D. Franceschi, Nat. Nanotech. **9**, 79 (2014).
- <sup>24</sup> R. Žitko, J. S. Lim, R. López, and R. Aguado, arXiv:1405.6084 (2014).
- <sup>25</sup> E. J. H. Lee, X. Jiang, R. Aguado, G. Katsaros, C. M. Lieber, and S. De Franceschi, Phys. Rev. Lett. **109**, 186802 (2012).
- <sup>26</sup> A. D. K. Finck, D. J. Van Harlingen, P. K. Mohseni, K. Jung, and X. Li, Phys. Rev. Lett. **110**, 126406 (2013).
- <sup>27</sup> H. O. H. Churchill, V. Fatemi, K. Grove-Rasmussen, M. T. Deng, P. Caroff, H. Q. Xu, and C. M. Marcus, Phys. Rev. B **87**, 241401 (2013).
- <sup>28</sup> E. Prada, P. San-Jose, and R. Aguado, Phys. Rev. B **86**, 180503(R) (2012).
- <sup>29</sup> G. Kells, D. Meidan, and P. W. Brouwer, Phys. Rev. B **86**, 100503 (2012).
- <sup>30</sup> T. D. Stanescu and S. Tewari, Phys. Rev. B **87**, 140504 (2013).
- <sup>31</sup> T. D. Stanescu and S. Tewari, arXiv:1310.4175 (2013).
- <sup>32</sup> D. A. Ivanov, Phys. Rev. Lett. **86**, 268 (2001).
- <sup>33</sup> J. Alicea, Y. Oreg, G. Refael, F. von Oppen, and M. P. A. Fisher, Nat. Phys. **7**, 412 (2011).
- <sup>34</sup> H. Kwon, K. Sengupta, and V. Yakovenko, Eur. Phys. J. B **37**, 349 (2003).
- <sup>35</sup> L. Fu and C. L. Kane, Phys. Rev. B **79**, 161408 (2009).
- <sup>36</sup> C. H. Lin, J. D. Sau, and S. Das Sarma, Phys. Rev. B **86**, 224511 (2012).
- <sup>37</sup> G. Ben-Shach, A. Haim, I. Appelbaum, Y. Oreg, A. Yacoby, and B. I. Halperin, (2014), 1406.5172.
- <sup>38</sup> Y. Oreg, G. Refael, and F. von Oppen, Phys. Rev. Lett. **105**, 177002 (2010).
- <sup>39</sup> T. Kato, *Perturbation theory for linear operators*, Vol. 132 (Springer, 1995).
- <sup>40</sup> N. Moiseyev, *Non-Hermitian Quantum Mechanics*, Vol. 1 (Cambridge University Press, 2011).
- <sup>41</sup> W. D. Heiss, J. Phys. A **45**, 444016 (2012).
- <sup>42</sup> W. D. Heiss, Phys. Rev. E **61**, 929 (2000).
- <sup>43</sup> R. Jackiw and C. Rebbi, Phys. Rev. D **13**, 3398 (1976).
- <sup>44</sup> A. Altland and M. R. Zirnbauer, Phys. Rev. B **55**, 1142 (1997).
- <sup>45</sup> A. P. Schnyder, S. Ryu, A. Furusaki, and A. W. W. Ludwig, Phys. Rev. B **78**, 195125 (2008).
- <sup>46</sup> S. Tewari and J. D. Sau, Phys. Rev. Lett. **109**, 150408 (2012).
- <sup>47</sup> J. Zak, Phys. Rev. Lett. **62**, 2747 (1989).
- <sup>48</sup> J. S. Lim, L. Serra, R. López, and R. Aguado, Phys. Rev. B **86**, 121103 (2012).
- <sup>49</sup> D. Rainis, L. Trifunovic, J. Klinovaja, and D. Loss, Phys. Rev. B **87**, 024515 (2013).
- <sup>50</sup> S. Das Sarma, J. D. Sau, and T. D. Stanescu, Phys. Rev. B **86**, 220506 (2012).
- <sup>51</sup> D. Pikulin and Y. Nazarov, JETP Letters **94**, 693 (2012).
- <sup>52</sup> D. I. Pikulin and Y. V. Nazarov, Phys. Rev. B **87**, 235421 (2013).
- <sup>53</sup> S. Das and I. I. Satija, (2014), 1409.6139.
- <sup>54</sup> J. Alicea, Rep. Prog. Phys. **75**, 076501 (2012).
- <sup>55</sup> D. Rainis and D. Loss, (2014), 1407.8239.
- <sup>56</sup> S. Mi, D. I. Pikulin, M. Marciani, and C. W. J. Beenakker, (2014), 1405.6896.
- <sup>57</sup> P. A. Ioselevich and M. V. Feigel'man, New Journal of Physics **15**, 055011 (2013).
- <sup>58</sup> Note that, in keeping with general scattering theory results<sup>52,57,62,63</sup>, the zero bias  $dI/dV$  is always zero, since the S-matrix topology is only effectively non-trivial.
- <sup>59</sup> S. W. Kim, Fortschritte der Physik **61**, 155 (2013).
- <sup>60</sup> C. Beenakker, in *Transport phenomena in mesoscopic systems: proceedings of the 14th Taniguchi symposium, Shima, Japan, November 10-14, 1991* (Springer-Verlag, 1992) p. 235.
- <sup>61</sup> P. San-Jose, E. Prada, and R. Aguado, Phys. Rev. Lett. **108**, 257001 (2012).
- <sup>62</sup> B. Béri, Phys. Rev. B **79**, 245315 (2009).
- <sup>63</sup> D. I. Pikulin, J. P. Dahlhaus, M. Wimmer, H. Schome-rus, and C. W. J. Beenakker, New Journal of Physics **14**, 125011 (2012).